THE REACTION $p + p \rightarrow p + p + \pi^0$ IN THE ENERGY RANGE FROM THRESHOLD TO 665 Mev*

A. F. DUNAĬTSEV and Yu. D. PROKOSHKIN

Joint Institute for Nuclear Research

Submitted to JETP editor December 25, 1958

J. Exptl. Theoret. Phys. (U.S.S.R.) **36**, 1656-1671 (June, 1959)

The angular distributions of π^0 mesons produced in proton-proton collisions have been investigated at 400 — 665 Mev. The distributions were found to be close to isotropic, in agreement with S. Mandel'shtam's phenomenological resonance theory. The total cross sections were measured in the energy range 313 — 665 Mev. At energies above 400 Mev the main contribution to the reaction cross section is made by resonant transitions. At lower proton energies the non-resonant Ss transition becomes significant, its contribution to the total cross section being $0.032\ \eta_m^2 \times 10^{-27}$ cm^2 (where η_m is the maximum π^0-meson momentum in the c.m.s.). A comparison of the measured cross sections of neutral and charged pions with the cross sections calculated from the resonance theory indicates that the transition with the total angular momentum $J = 2$ plays the predominant role.

1. INTRODUCTION

THE production of neutral pions in proton collisions

$$p + p \rightarrow p + p + \pi^0, \qquad \pi^0 \rightarrow 2\gamma \tag{1}$$

occupies a prominent place among the reactions of the type "nucleon plus nucleon → pion." Its distinguishing feature is the rapid increase in the cross section with energy and the relatively small value of the cross section near the threshold, which is a consequence of the forbiddenness of a transition with a final state S for the nucleons and a final state p for the pion relative to the center of mass, a transition that plays a principal role in other meson-production reactions (the Sp transition in the Rosenfeld classification[1]). The first investigations of this reaction[2-8] have shown that in the energy range 340 — 480 Mev its cross section $\sigma_{pp}^{\pi^0}$ increases as η_m^8 (where η_m is the maximum π^0-meson momentum in the c.m.s.), measured in units of meson mass $m_\pi c$), while other reactions are characterized by cross sections that depend on powers of η_m not higher than the fourth. A phenomenological analysis of these data[1,9] has shown that near threshold the reaction (1) is essentially caused by the Pp transition. It has been noted in later papers[6,10,11] that the cross section $\sigma_{pp}^{\pi^0}$ continues to increase rapidly even at 450 — 660 Mev: $\sigma_{pp}^{\pi^0} \sim \eta_m^{4.5}$ according to Soroko[6] and $\sigma_{pp}^{\pi^0} \sim \eta_m^{5.5}$ according to Prokoshkin and Tyapkin.[11] A comparison of the data of Mather and Martinelli[7] or those of Crandall and Moyer[8] with the results of Prokoshkin and Tyapkin[11] shows that at lower energies the cross section varies as η_m^6 and not as η_m^8, from which it has been concluded[11] that the Ss transition plays a substantial role at low energies. Further measurements of the cross section of the reaction (1) at low energies[12] have confirmed this conclusion.

The experimental data obtained in reference 11 were analyzed by Mandel'shtam within the framework of the phenomenological resonance theory.[13] In contrast with the old phenomenological theory[1,9] Mandel'shtam considers the resonant interaction of the pion with the nucleon in the final state of the reaction. It is assumed in his theory that over a wide energy range, where the resonant interaction between the meson and the nucleon is substantial, the matrix elements of the transitions are constant to within factors that consider the meson-nucleon and nucleon-nucleon interaction in the final state. The theory takes into account the interference of nucleon states and "shifted" transitions.[7] The S scattering of the system, when one of the nucleons is in the S state with respect to the meson-nucleon subsystem, for which one possible state $^2P_{3/2}$ is assumed, is described in this case by a single parameter, while

*The results of this investigation were reported at the Fourth Session of the Scientific Council of the Joint Institute for Nuclear Research in May 1958.

the P scattering is described by five parameters. The theory was found to be not critical to relative changes in the parameters of the P scattering, which made it possible to equate some of these parameters to each other and thus reduce the experimentally-determined number of P-scattering parameters from 5 to 2. All three parameters that describe the S and P scattering are determined from the experimental data on the production of charged pions in p-p collisions. The total cross sections of the reaction (1) are calculated in the Mandel'shtam theory without introducing any supplementary free parameters, thus making the comparison of the experimental and theoretical energy dependences of this cross section a good test of the resonance theory. A corresponding comparison with the data of Prokoshkin and Tyapkin,[11] made by Mandel'shtam, has shown an agreement between the experimental and theoretical results.

The angular distribution of π^0 mesons in reaction (1), calculated on the basis of the resonance theory, is close to isotropic at all proton energies. Experiments carried out by various methods in the region near 600 Mev[11,14,15] actually indicate that the angular distribution of the π^0 mesons is isotropic. However, at lower energies (450 — 550 Mev) the measured angular distributions have displayed a tendency towards increased anisotropy.[11] In the range of even lower energies, the angular distribution was analyzed by Moyer and Squire[16] under certain assumptions concerning the character of the π^0-meson spectrum, based on the old phenomenological theory.[1,9] Within the framework of these assumptions, they conclude that the angular distribution of the π^0 mesons is substantially anisotropic at 330 Mev.

The purpose of this work was to investigate the reaction (1) over a wide energy interval. The use of a single procedure gave grounds for hoping to be able to obtain sufficiently accurate data on the variation of the reaction characteristics with the energy. Particular attention was paid to a little-studied characteristic of the reaction — the angular distribution of the π^0 mesons. In investigations of this type it is necessary to take into account the inherent difficulties connected with the fact that the π^0 mesons move at a velocity substantially different from that of light. This causes the angular distribution of the gamma quanta, produced during the decay of the π^0 mesons, to be less anisotropic than the distribution of the π^0 mesons.[17] As the velocity of the π^0 mesons decreases, the anisotropy of the angular distribution of the gamma quanta disappears rapidly. The foregoing is demonstrated in Fig. 1, which illustrates the case when π^0 mesons are distributed proportional to $\frac{1}{3} + b_{\pi 0} \cos^2 \vartheta$ in the c.m.s. Here the angular distribution of the gamma quanta is of the form $\frac{1}{3} + b_\gamma \cos^2 \vartheta$. The figure shows the value of db_{π^0}/db_γ i.e., the error in the measurement of $b_{\pi 0}$, at various energies E_p of the protons that produce the π^0 mesons. It is seen that when E_p decreases this error increases rapidly, consequently increasing the accuracy with which it is necessary to measure the angular distribution of the gamma quanta so as to establish the angular distribution of the π^0 mesons. It is also necessary to take into account the fact that when the proton energy decreases, the more stringent requirements regarding the measurement accuracy are accompanied by an exceedingly rapid reduction in the yield of the gamma quanta from the investigated reaction. This complicates even further the investigation of the angular distributions of the π^0 mesons. In the present investigation we restricted ourselves to a measurement of the angular distributions of gamma quanta in the interval 400 — 665 Mev, where the aforementioned difficulties were not yet too great and the apparatus employed made it possible to determine with sufficient accuracy the angular distribution of the π^0 mesons.

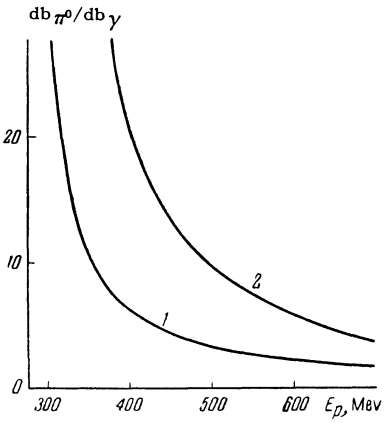

FIG. 1. Dependence of the relative error db_{π^0}/db_γ on the proton energy: 1) For $b_{\pi^0} \approx 0$; 2 — for $b_{\pi^0} = 1$.

2. MEASUREMENT PROCEDURE

Proton beam. The experiments were performed on the external unpolarized proton beam of the six-meter synchro-cyclotron of the Joint Institute for Nuclear Research. The proton current was measured accurate to 3% with a calibrated helium-filled ionization chamber. Since the cross section of the investigated reaction depends considerably on the proton energy, particularly near threshold, the cross-section measurements must be accompanied by an exact determination of the mean energy of the beam. At small proton energies, on the

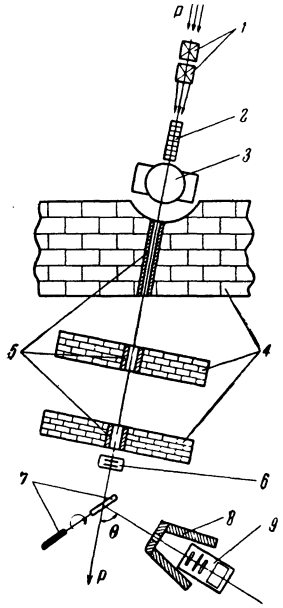

FIG. 2. Arrangement of the apparatus: 1) focusing magnetic lenses, 2) polyethylene absorber, 3) deflecting magnet, 4) shielding walls, 5) steel collimators, 6) ionizing chamber, 7) targets, 8) portion of lead shielding of the gamma telescope, 9) gamma telescope, P – proton beam.

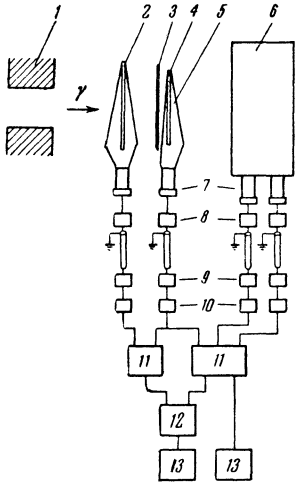

FIG. 4. Diagram of the gamma telescope: 1) lead diaphragm, 2) crystal of anti-coincidence counter, 3) converter, 4) crystal of coincidence counter, 5) foil used to reflect light, 6) radiator of the Cerenkov counter, 7) photomultipliers, 8) shaping stages, 9) cathode follow ups, 10) amplifiers, 11) coincidence circuits, 12) anti-coincidence circuits, 13) scalers.

other hand, it is necessary to measure accurately not only the mean energy, but also the energy spectrum of the beam. The mean energy of the beam was determined in these experiments with accuracy to approximately 1 Mev by the method described in reference 18. The proton energy was reduced by means of polyethylene blocks located in front of the shielding wall (Fig. 2). The energy distributions of the beam protons fits well a Gaussian curve with a dispersion of 2.8 ± 0.3 Mev at maximum proton energy. The dispersion increased with deceleration of the beam, as seen in Fig. 3.

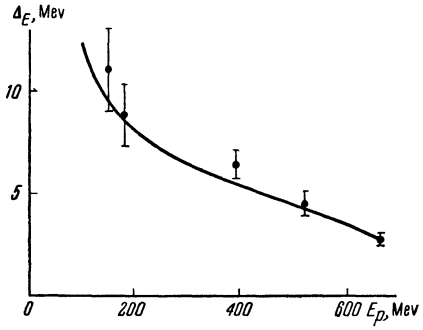

FIG. 3. Dispersion of the beam Δ_E at various proton energies E_p.[18] Solid curve – theoretical dependence of the dispersion on the energy, calculated with allowance for the ionization losses and a "straggling" type of dispersion.

Recording apparatus. Information on the angular distribution of the π^0 mesons and on the value of the total cross section was obtained by registering the gamma quanta from the decay of π^0 mesons, produced in the target by the passage of the proton beam. The gamma quanta were registered with a counter telescope shown schematically in Fig. 4.

The gamma quanta produced in the target were collimated with the aid of a lead diaphragm and fell on the telescope lead converter, where they produced electron-positron pairs. The pairs were registered by a scintillation counter and Cerenkov counter connected for coincidence. Because of the small thickness of the converter (0.5 — 2 mm) and of the scintillators (3 mm) and because of the "broad geometry" of the telescope and the absence of absorbers between the counters, the gamma telescope had a low energy threshold and could register effectively gamma quanta with energies down to 10 Mev. The telescope was made insensitive to either neutrons or charged particles by using a scintillation counter placed in front of the converter and connected for anti-coincidence with the other telescope counters. The counting rate of the telescope placed in the gamma beam was increased 25 fold by placing in it a converter 2 mm thick. Increasing the converter thickness to 5 mm improved this ratio to 40. The telescope could be operated at a relatively large extraneous-radiation background by using coincidence circuits with a time resolution of 10^{-8} sec.

In most of the earlier investigations the efficiency of the gamma telescope was determined by measuring or calculating the sensitivity of the gamma telescope to gamma quanta of various energies, from which the efficiency was found by integrating this energy curve simultaneously with the theoretically-obtained gamma spectra. Consequently the results in these investigations were substantially dependent on the correctness of the theoretical assumptions concerning the gamma spectrum, particularly in those cases[6,16] when the measurements were made with a detector having a high energy threshold. In the present investigation the efficiency was determined experimentally by a method[11] that permitted a determination of

the gamma-quantum yield without making any assumptions concerning their energy spectrum. The dependence of the telescope efficiency w on the angle θ (see Fig. 2), measured at proton energies of 665 and 485 Mev, is shown in Fig. 5. At other

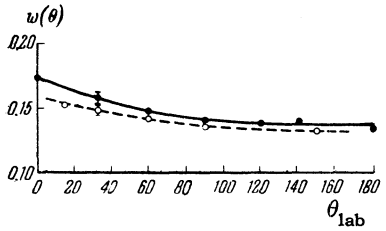

FIG. 5. Efficiency of gamma telescope, w; ● – at E = 665 Mev, o – at E = 485 Mev.

energies the dependence $w(\theta)$ has a similar character. As the proton energy decreases, the efficiency decreases and simultaneously, the shape of the $w(\theta)$ curve also changes, because of the reduction in the π^0-meson energy and the velocity of the center-of-mass system. Efficiency measurements made at 665 Mev with graphite, polyethylene, and liquid-hydrogen targets have shown that w is the same for hydrogen and carbon. This result is the consequence of the low energy threshold of the gamma telescope. In spite of the great difference between the gamma spectra at $\theta = 0°$ and $\theta = 180°$ (reference 19) (the mean energies of the spectra are 190 and 75 Mev) the efficiencies $w(0°)$ and $w(180°)$ differ by merely 25%. There is a much smaller difference between the spectra measured for carbon at hydrogen at a single angle,[15,19] and consequently the corresponding efficiencies are also close. As the proton energy decreased, the difference in the efficiency for hydrogen and carbon increased somewhat, but in the investigated energy range this difference still did not influence the results of the measurements, since it was much less than the statistical accuracy of the measured ratio of the gamma yields at different angles. The latter made it possible to use the functions $w(\theta)$, measured for carbon, to find the angular distribution of the gamma quanta from reaction (1) at low proton energies.

Targets. Control experiments. The target used was liquid hydrogen, sealed in a container made of foamed polystyrol. The target was in the form of a cylinder 8 cm in diameter and 25 cm long, so placed that the beam, traveling parallel to the cylinder axis, did not strike the side walls of the target (the beam was 6 cm wide). The conditions for registering the gamma quanta were most favorable in the angle interval $45° < \theta < 145°$. In this case the lead diaphragm, placed in front of the telescope, prevented the gamma radiation from the entrance and exit windows of the target from entering the telescope, and the telescope registered only the gamma radiation from the hydrogen. When the hydrogen was removed from the container, the counting rate of the telescope was decreased to one-tenth at an energy of 660 Mev.

The cross section of reaction (1) was also determined by a differential method, by irradiating targets made of polyethylene and graphite. These targets were approximately 3g/cm^2 thick and were chosen such that the beam-energy loss in the target was the same. The polyethylene and graphite targets were placed at an angle of 45° to the proton beam, as shown in Fig. 2, and were introduced into the beam alternately. The targets were changed every 1 – 3 minutes, to eliminate the influence of the change in sensitivity of the registering apparatus on the measurement accuracy. In spite of the fact that ethylene contains only 14% hydrogen, in many cases the difference method yielded a much higher accuracy then the use of liquid hydrogen targets. The reason for this was the difficulty of accurate determination of the effective volume of the liquid-hydrogen target in which the gamma quanta registered by the telescope were produced. Liquid hydrogen was therefore used usually to make accurate relative measurements, while the absolute measurements were made by the differential method.

To obtain a sufficiently high counting rate, the telescope was placed close to the target. This caused the gamma radiation from the various sections of the target to be registered by the telescope with unequal efficiency, and consequently the efficiency of the registration depended on the dimensions of the target. This efficiency, which depends on the dimensions of the target, will be called in the future the form factor of the target. The graphite target was made of light graphite of density 0.9 g/cm^3, and consequently the form factors of the polyethylene and graphite targets differed little. The maximum difference in the form factors for the used targets amounted to 1.5% at $\theta = 90°$, and decreased rapidly with decreasing θ. Since the ratios of the gamma yields from the targets should be measured with accuracy to 1%, great attention was paid to the determination of the form factors of the targets. The form factors were determined experimentally at different angles θ, with accuracy better than 0.5%. Many control experiments, performed with targets of different shapes, have shown good agreement between the measured and calculated form factors. The basic and most laborious control experiment was carried out at a proton energy of 275 Mev. Since this energy is below the threshold of production of π^0 mesons in p-p

TABLE I

θ°	σ'_{pp}, %	θ°	σ'_{pp}, %	θ°	σ'_{pp}, %	θ°	σ'_{pp}, %
$E = 665$ Mev		$E = 665$ Mev		$E = 560$ Mev		$E = 485$ Mev	
16	14.7±0.8	96	10.8±0.5	16	9.9±0.6	16	5.1±1.0
20	15.4±0.8	120	9.9±0.4	34	9.4±0.9	35	5.3±0.5
33	14.9±0.5	135	9.2±0.8	60	7.5±0.7	60	5.6±0.8
45	14.5±0.8	145	9.4±1.2	90	6.8±0.5	90	4.4±0.7
60	12.7±0.6	160	10.0±1.2	130	6.4±1.0	130	4.0±0.7
75	11.6±0.8			150	6.0±0.7	150	4.5±0.9

collisions, the ratio of the cross sections for hydrogen and carbon measured by the differential method should be zero, if the form factors have been accurately determined. Experiment actually yielded value close to zero:

$$(\sigma^{\gamma}_{pp} / \sigma^{\gamma}_{pC})_{\text{meas}} = -0.001 \pm 0.006.$$

3. MEASUREMENT RESULTS

Angular distributions of gamma quanta. In the region of large proton energies, the angular distributions of the gamma quanta were investigated both by the differential method and by the use of liquid hydrogen. In the former case the measurements were performed in two stages: the angular distribution of the gamma quanta produced in collisions between protons and carbon nuclei, $f_{pC}(\vartheta)$ were measured, after which the ratio of the differential cross sections for hydrogen and carbon were found for each angle of observation:

$$\sigma'_{pp} = (d\sigma^{\gamma}_{pp} / d\Omega) / (d\sigma^{\gamma}_{pC} / d\Omega).$$

The angular distribution of the gamma quanta produced on carbon by protons with E = 665 Mev* is shown in Fig. 6. The angular distributions $f^{\gamma}_{pC}(\vartheta)$ at lower energies are similar in form.

The relative cross sections σ'_{pp} were measured by the differential method at energies E = 665, 560, and 485 Mev for a large number of values of θ (see Table I). So detailed an investigation of the function $f^{\gamma}_{pp}(\vartheta)$ was undertaken to verify whether the measurement method employed is accompanied by some noticeable systematic errors. The distribution of the gamma quanta formed in p-p collisions should be symmetrical about $\vartheta = 90°$ in the c.m.s., in view of the indistinguishability of the colliding particles. Any deviation from symmetry in the measured distribution must therefore be considered as an indication of the presence of systematic errors in the procedure.

*Here and below E denotes the effective energy of the beam, determined with allowance for the energy loss in the target and the dispersion of the beam.

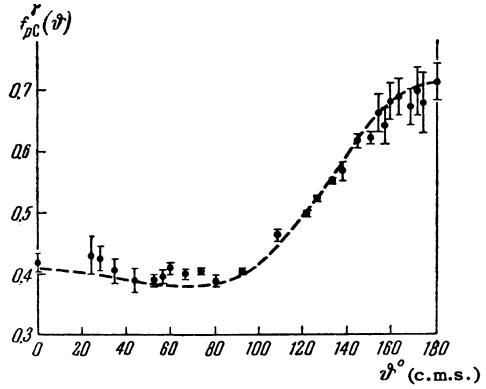

FIG. 6. Angular distribution of gamma quanta produced on carbon by 665 Mev protons. Dotted curve is calculated on the basis of the optical model of the nucleus.[14]

The angular distribution of gamma quanta obtained from the data of Fig. 6 and Table I at E = 665 Mev is shown in Fig. 7. It is represented by the polynomial

$$f^{\gamma}_{pp}(\vartheta) \sim \tfrac{1}{3} + (0.07 \pm 0.02)\cos^2\vartheta.$$

This function, found by the least-squares method and normalized in a suitable manner, is shown dotted in Fig. 7. The angular distribution of the gamma quanta we obtained was found to be symmetrical. If it is approximated by a polynomial that contains, along with the zero and second-order term, also an asymmetric term proportional to $\cos\vartheta$, the contribution of the latter is found to be insignificant: $(0.009 \pm 0.011)\cos\vartheta$. An analysis of the distribution $f^{\gamma}_{pp}(\vartheta)$, measured at E = 665 Mev, shows also that the contribution of the

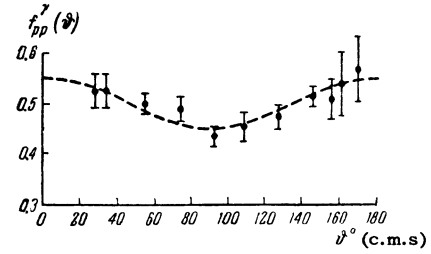

FIG. 7. Angular distribution of gamma quanta from reaction (1) at E = 665 Mev, measured by the differential method. The dotted curve was found by the least-squares method.

cosine powers higher than the second is insignificant: the fraction of gamma quanta distributed in proportion to $\cos^4\vartheta$ amounts to merely (0.015 ± 0.030). The same should also occur at lower proton energies, since the role of the states with large moments diminishes as the reaction threshold is approached. One can therefore assume that in the energy interval $E \lesssim 660$ Mev the gamma quanta from the reaction (1) have the following angular distribution in the c.m.s.

$$f^{\gamma}_{pp}(\vartheta) \sim \tfrac{1}{3} + b_{\gamma}\cos^2\vartheta. \qquad (2)$$

To determine the values of b_γ it is enough to find the ratio of the gamma yields at two angles. Similar measurements were carried out at energies less than 616 Mev, essentially with a liquid-hydrogen target, since the differential method yields accurate values of b_γ only for $E \approx 600$ Mev, as seen from Figs. 7 and 8. The gamma

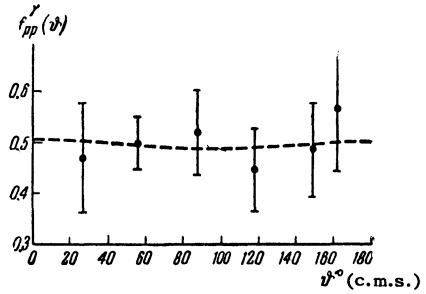

FIG. 8. Angular distribution of gamma quanta from reaction (1) at E = 485 Mev, measured by the differential method. The dotted curve was found by the least-squares method and corresponds to $f^{\gamma}_{pp}(\vartheta) \sim \frac{1}{3} + 0.02\cos^2\vartheta$.

yields were measured at angles $\theta_1 = 55$ to 60° and $\theta_2 = 120$ to 125°. The values of θ_1 and θ_2 varied little with decreasing E. The angles θ_1 and θ_2 were chosen complementary in order to avoid the difficulties connected with the determination of the effective volume of the liquid-hydrogen target. The indicated values of θ_1 and θ_2 are convenient because they correspond to the c.m.s. angles $\vartheta_1 = 90°$ and $\vartheta_2 = 145°$, for which the differential cross sections are connected with the total cross section by the simple relation

$$\sigma^{\pi^0} = \pi\{d\sigma^{\gamma}(\vartheta_1)/d\Omega + d\sigma^{\gamma}(\vartheta_2)/d\Omega\}, \qquad (3)$$

which holds for all values of b_γ. At energies E > 500 Mev, the measurements of b_γ were carried out both with the liquid-hydrogen target and the differential method. In the latter case the gamma yields were measured at several angles, including θ_1 and θ_2. The values of b_γ found by the various methods are the same, within the limits of measurement errors. The values obtained for b_γ are listed in Table II.

TABLE II

E, Mev	b_γ	E, Mev	b_γ
665	0.050±0.017	517	0.05±0.06
630	—0.02±0.04	485	0.01±0.04
590	0.06±0.05	440	—0.01±0.06
560	0.02±0.03	400	0.015±0.060

Determination of the angular distribution of the π^0 mesons. The angular distributions of the π^0 mesons can be determined from the measured angular distributions of the gamma quanta. Let us show first how this problem is solved in the case when the π^0 mesons are monoenergetic. Let the π^0 mesons have a velocity β, and let their angular distribution be described in the c.m.s. by the function $V(\cos\vartheta, \varphi)$. The angular distribution of the gamma quanta from the decay of the π^0 mesons, $F(\cos\vartheta, \varphi)$ is determined by the integral equation

$$F(\cos\vartheta, \varphi) = (\xi^2 - 1)\int_{-1}^{1}\int_{0}^{2\pi} V(\cos\vartheta_0, \varphi_0)[\xi - \cos\vartheta\cos\vartheta_0 - \sin\vartheta\sin\vartheta_0\cos(\varphi - \varphi_0)]^{-2} d\cos\vartheta_0 d\varphi_0. \qquad (4)$$

Here $\xi = 1/\beta$. We shall restrict ourselves in the future to the very general case, when the angular distribution of the π^0 mesons is independent of the azimuth angle φ. Then, integrating (4) over φ_0, we get

$$F(\cos\vartheta) = \tfrac{1}{2}(\xi^2 - 1)\int_{-1}^{1} V(\cos\vartheta_0)\, G(\cos\vartheta, \cos\vartheta_0)\, d\cos\vartheta_0. \qquad (5)$$

The kernel of Eq. (5) is symmetrical:

$$G(\cos\vartheta, \cos\vartheta_0) = (\xi - \cos\vartheta\cos\vartheta_0)[(\cos\vartheta + \cos\vartheta_0)^2 - (\xi + 1)(2\cos\vartheta\cos\vartheta_0 - \xi + 1)]^{-3/2}.$$

Formula (5) makes it possible to determine the angular distribution of the π^0 mesons, $V(\cos\vartheta)$, provided the angular distribution of the gamma quanta is known. A solution of this problem can be obtained either by reducing Eq. (5) to a system of linear equations, or by expanding Eq. (5) in eigenfunctions (the eigenfunctions of these equations are Legendre polynomials $P_n(\cos\vartheta)$, which follows from (4) if the "addition theorem" for the Legendre polynomial is used). In the latter case, replacing $F(\cos\vartheta)$ by the series $\Sigma a_n P_n(\cos\vartheta)$, we find

$$V(\cos\vartheta) = \sum_n \frac{a_n}{\alpha_n(\xi)} P_n(\cos\vartheta). \qquad (6)$$

The eigenvalues $\alpha_n(\xi)$ can be readily obtained by using the Neumann formula for the Legendre polynomials

$$\alpha_n(\xi) = (1-\xi^2)\,Q_n'(\xi), \tag{7}$$

where $Q_n'(\xi)$ is the derivative of the Legendre function of the second kind:

$$Q_n(\xi) = P_n(\xi)\,\tanh^{-1}\frac{1}{\xi} - \sum_{k=0}\frac{2n-4k-1}{(2k+1)(n-k)}\,P_{n-2k-1}(\xi).$$

The above relations determine the angular distribution of monoenergetic π^0 mesons. This problem becomes more complicated if the π^0 mesons are not monoenergetic. In the most general case, when the distribution function of the π^0 mesons, $U(\cos\vartheta, \xi)$, cannot be separated into angle and energy factors, and it becomes necessary to investigate both the angle and the energy distribution of the gamma quanta in order to determine the distribution $U(\cos\vartheta, \xi)$. In the case when the angular and energy variables can be separated, i.e., when

$$U(\cos\vartheta, \xi) = V(\cos\vartheta)\,R(\xi), \tag{8}$$

the function $V(\cos\vartheta)$ can be determined by finding the average eigenvalues $\overline{\alpha}_n$, which are obtained by averaging the functions (7) over the spectrum $R(\xi)$. To carry out such an averaging in the general case it is necessary to know the spectrum $R(\xi)$. However, if the angular distribution of the gamma quanta differs little from isotropic, it is enough to have only tentative information on the spectrum, which can be obtained from the kinematics of the reaction (1). This last circumstance was used in the present work 4, as seen from Table II, the measured angular distributions of the gamma quanta are close to isotropic. In finding the angular distribution of the π^0 mesons it was assumed that the distribution function could be represented in form (8). As follows from (2) and (6), the angular distribution of the π^0 mesons has the form

$$f_{pp}^{\pi^0}(\vartheta) \sim \tfrac{1}{3} + b_{\pi^0}\cos^2\vartheta. \tag{9}$$

The values of b_{π^0} for various proton energies are listed in Table III.

TABLE III

E, Mev	b_{π^0}	E, Mev	b_{π^0}
665	0.10±0.03	517	0.13±0.15
630	−0.04±0.08	485	0.02±0.12
590	0.14±0.12	440	−0.03±0.16
560	0.04±0.07	400	$0.07^{+0.40}_{-0.25}$

Total cross sections of reaction (1). At a proton energy E = 660 Mev, we measured the differential cross section for the production of gamma quanta on carbon at θ = 33°. Its value is

$$d\sigma_{pC}^{\gamma}(33°,\ 660\ \text{mev})/d\Omega = (7.6\pm0.4)\cdot10^{-27}\ \text{cm}^2/\text{sterad}$$

and is in good agreement with the cross section measured with the internal beam of the accelerator.[11] Integration of the resultant angular distributions of the gamma quanta, normalized to the aforementioned cross section, gives the value of the total cross section of the reaction (1):

$$\sigma_{pp}^{\pi^0}(660\ \text{Mev}) = (3.22\pm0.17)\cdot10^{-27}\ \text{cm}^2.$$

In experiments with a liquid-hydrogen target we obtain the nearly-equal value

$$(3.4\pm0.4)\cdot10^{-27}\ \text{cm}^2.$$

The dependence of the total cross section of reaction (1) on the proton energy was measured by us in the interval 313 — 665 Mev. The gamma yields were measured at several angles, including the "isotropic" angles[11,17,20] (33 and 96° in the laboratory system at E = 660 Mev), and also at the angles θ_1 and θ_2, which made it possible to determine simply the ratio of the total cross sections at different proton energies. In determining the cross sections by the differential method we used the energy relations for the cross sections of carbon, measured at the "isotropic" angles. One of these is shown in Fig. 9. The relative cross sections σ'_{pp} were determined by the differential method at energies E ≳ 400 Mev (see Table IV). At lower energies, the measurements were carried out only with liquid hydrogen. The relative cross sections σ'_{pp}, obtained by comparing the energy relationships of the cross section for the hydrogen (liquid-hydrogen target) in carbon, are

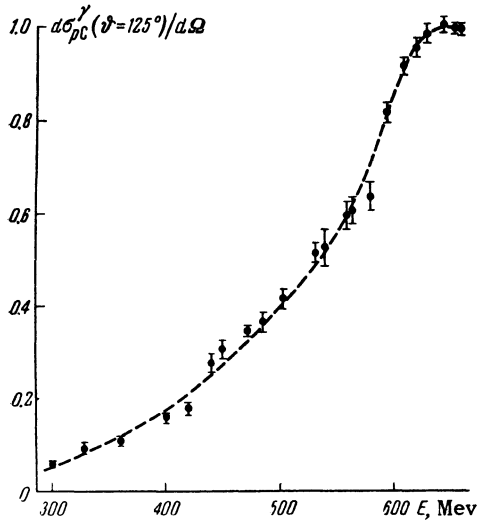

FIG. 9. Dependence of the cross section for production of gamma quanta on carbon on the proton energy (in relative units).

TABLE IV

E, Mev	$\sigma'_{pp}(\vartheta = 125°)$, %		E, Mev	$\sigma'_{pp}(\vartheta = 125°)$, %	
	differential method	liquid hydrogen		differential method	liquid hydrogen
660	10.8± 0.6	10.8±0.6	400	1.3±0.4	1.6±0.3
645	—	10.0±0.6	377	—	1.0±0.3
630	9.3 ±0.6	8.7±0.6	360	—	0.9±0.3
610	—	7.6±0.5	350	—	0.7±0.2
590	9.1 ±0.4	7.5±0.6	340[7]	—	0.6±0.1
560	6.8 ±0.5	6.5±0.5	328	—	0.5±0.2
517	5.5 ±0.5	5.0±0.5	313	—	0.3±0.2
485	4.4 ±0.7	3.8±0.4	295	—	<0.3
445	2.9 ±0.5	2.1±0.3			

TABLE V

E, Mev	$\sigma^{\pi^0}_{pp}$		η_m	E, Mev	$\sigma^{\pi^0}_{pp}$		η_m
	Relative units	10^{-27} cm^2			Relative units	10^{-27} cm^2	
665	1.01±0.01	3.24±0.18	1.90	507	0.22±0.01	0.71±0.05	1.38
660	1.00	3.22±0.17	1.89	485	0.139±0.006	0.45±0.03	1.30
652	0.93±0.03	3.00±0.18	1.86	458	0.093±0.008	0.30±0.03	1.19
645	0.91±0.02	2.93±0.17	1.84	445	0.063±0.004	0.20±0.02	1.14
638	0.90±0.03	2.90±0.18	1.82	412	0.039±0.005	0.12±0.02	1.00
630	0.85±0.02	2.74±0.16	1.79	400	0.027±0.004	0.09±0.02	0.95
622	0.81±0.03	2.61±0.17	1.77	374	0.012±0.003	0.04±0.01	0.83
610	0.70±0.02	2.25±0.13	1.73	360	0.009±0.003	0.030±0.008	0.75
597	0.61±0.03	1.96±0.13	1.69	350	0.006±0.002	0.018±0.006	0.70
590	0.57±0.02	1.84±0.13	1.66	328	0.004±0.002	0.014±0.006	0.58
560	0.385±0.013	1.24±0.07	1.56	313	0.002±0.001	0.006±0.004	0.48
531	0.26±0.01	0.84±0.06	1.46	295	<0.001	<0.004	0.32

also given in Table IV. The values σ'_{pp} were normalized in this case to E = 660 Mev. The dependence of the total cross section of reaction (1) on the energy E is given in Table V. The total cross sections listed in the same table were obtained by normalizing the energy dependence of the cross section $\sigma^{\pi^0}_{pp}$ to that measured at E = 660 Mev. To determine the energy dependence of the total cross section we used the data of Fig. 9 and Table IV, and also analogous data obtained by measuring the gamma yields at other angles.

As can be seen from Table V the gamma yield decreases by nearly 500 times with decreasing proton energy in the investigated region. The cross section of reaction (1), measured at 313 Mev, is one-thirtieth the cross section of charged-pion production at the same energy. So small a magnitude of the observed effect makes it necessary to account thoroughly for all the extraneous gamma-radiation sources capable of competing with the investigated reaction. The effect of these sources was analyzed by Moyer and Squire[16] and was found to be insignificant in the investigated region. The greatest danger came in our case from contamination of the proton beam by neutrons knocked out from the polyethylene absorber, used to decelerate the beam. A series of control experiments, in which the slowed-down proton beam was either deflected with a magnet (see 3, Fig. 2), or completely stopped in a polyethylene absorber, has shown that the influence of the neutron admixture is insignificant. An estimate made on the basis of the known neutron yield from the inner target[21] also shows that the contribution due to the neutron admixture is small and amounts to not more than 3% of the cross section measured at E = 313 Mev. The measured gamma-yields can be almost completely attributed to reaction (1) in the investigated energy region. At energies closer to the reaction threshold than in our case, the hard gamma bremsstrahlung of the protons becomes more substantial, and its cross section, according to reference 22, is 10^{-30} cm^2.

4. DISCUSSION

Angular distributions of π^0 mesons. A characteristic feature of the π^0-meson angular distributions obtained in the present investigation is their isotropy over the entire investigated region of proton energies. The angular distributions of references 11 and 16 are more isotropic at low proton energies, as can be seen from Fig. 10. The same diagram shows the energy dependence of the quantity $\delta = 1/(1 + b_{\pi^0})$, which represents the

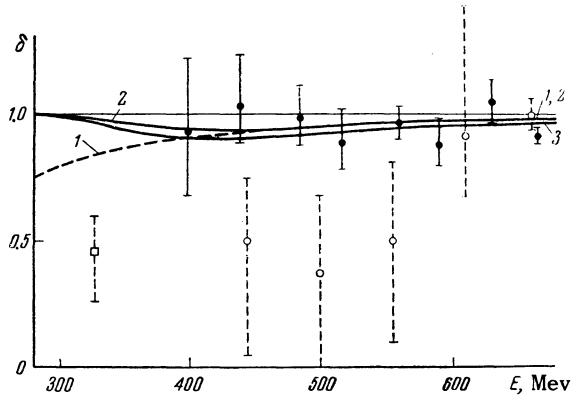

FIG. 10. Angular distributions of π^0 mesons in reaction (1) [the function $\delta(E) = 1/(1 + b_{\pi^0})$ where b_{π^0} is the coefficient in the distribution (9)]. ● – result of the present work, o – data of reference 11, □ – data of reference 16. The curves were calculated: 1) under the assumption of (10) without account of the nonresonant Ss transition; 2) the same, but with allowance for the Ss transition, the contribution of which is $0.032\ \eta_m^2 \times 10^{-27}$ cm^2; 3) assuming (11) with allowance for the Ss transition.

fraction of the π^0 mesons isotropically distributed if the angular distribution has the form of Eq. (9) and $b_{\pi^0} \geq 0$. The value of δ at E = 329 Mev has been determined with a detector having a high energy threshold[16] and depends therefore on the correctness of the theoretical assumptions made with respect to the distribution function of the π^0 mesons. On the other hand, the contemporary phenomenological theories[1,9,13] differ greatly in their conclusions concerning the distribution function of the π^0 meson in reaction (1). The experimentally determined values of δ are compared in Fig. 1 with the function $\delta(E)$, calculated by Mandel'shtam (private communication)* on the basis of the theory developed in reference 13. Curve 1 in this diagram is calculated with allowance for only resonant transitions. At large energies δ is close to unity. According to Mandel'shtam, this is due to predominance of P scattering over S scattering, the latter being practically supressed by interference. As the reaction threshold is approached, the anisotropy of the angular distribution of the π^0 mesons produced in resonant transitions increases. However, the contribution due to resonant transitions in this energy range is relatively small. What predominates in this case is the nonresonant Ss transition, which is characterized by an isotropic π^0-meson angular distribution. Therefore the dependence $\delta(E)$, calculated with allowance for the nonresonant Ss transition, is found to be close to unity in the entire investigated energy interval, in agreement with the results of the present work.

The values of δ given in Fig. 10 were determined by us from the experimental values of b_γ, under the assumption that the angle and energy components of the π^0-meson distribution function are independent [see Eq. (8)]. The Mandel'shtam theory, however, predicts that the anisotropy of the angular distribution of the π^0 mesons diminishes with their energy, and the coefficient b_{π^0} may even become negative near the lower boundary of the spectrum (thereby differing from references 1 and 9). Therefore, if δ is calculated from the data of Table II on the basis of spectra taken from the Mandel'shtam theory, they will be located somewhat closer to unity than shown in Fig. 10.

Energy dependence of the cross section of reaction (1). The total cross section measured in

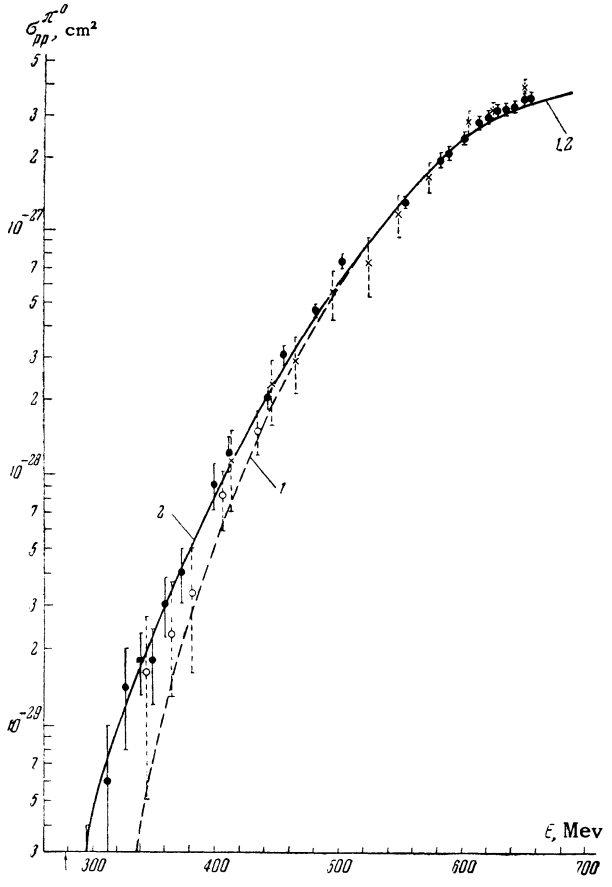

FIG. 11. Total cross sections of reaction (1). ● – results of the present work ■ – from data of the present work and reference 7, × – from data of reference 11, o – data of reference 12. The arrow indicates the reaction threshold. 1) resonant curve calculated in reference 13, 2) curve with account of the nonresonant Ss transition, the contribution of which to the total cross section is $0.032\ \eta_m^2 \times 10^{-27}$ cm^2.

*We take this opportunity to thank S. L. Mandel'shtam who graciously communicated to us the results of several of his unpublished calculations.

the present work are shown in Fig. 11. Along with our results, Fig. 11 shows the cross section, determined from our present data on the cross section for carbon and from the data of Mather and Martinelli[7] on the relative cross section σ'_{pp} (see Table IV). The total cross section obtained, $\sigma^{\pi^0}_{pp}$ (340 Mev) = (0.018 ± 0.005) × 10^{-27} cm^2, is almost double the cross section [(0.010 ± 0.003) × 10^{-27} cm^2] obtained earlier with the results of Mather and Martinelli and those of Crandall and Moyer,[8] and usually cited in earlier papers. This difference is caused by the discrepancy between the cross sections for carbon, measured in the present paper; [(3.0 ± 0.4) × 10^{-27} cm^2] and those of reference 8 [(1.7 ± 0.4) × 10^{-27} cm^2]. We shall show that the cross section for the production of charged pions on carbon at this energy is (7.5 ± 1.0) × 10^{-27} cm^2 (reference 23), from which it follows that $\sigma^{\pi^0}_{pC}$ = (3.7 ± 0.5) × 10^{-27} cm^2, if one uses the relation $\sigma^{\pi^+}_{pC} + \sigma^{\pi^-}_{pC} = 2\sigma^{\pi^0}_{pC}$, which follows from the hypothesis that the nuclear forces are independent of the charge, and which is found experimentally to be sufficiently accurate.[24]

As can be seen from Fig. 11, the cross sections measured by us agree, within the limits of experimental error, with the values previously obtained.[11] The cross sections measured at Carnegie[12] are somewhat lower than those of the present paper, possibly owing to the excessive value used in reference 12 for the efficiency of the gamma telescope. The efficiency calculated in that paper at large gamma energies exceeds the maximum value possible, namely $1-\exp(-\mu d)$ (μ is the coefficient of absorption of gamma quanta in the converter substance and d the thickness of the converter.

The total cross sections obtained by us are compared in Fig. 11 with the theoretical resonance curve of Mandel'shtam. This comparison shows that the behavior of the reaction cross section in the energy region near 600 Mev can be described quite accurately within the framework of a theory that takes only resonant transitions into account. At energies less than 500 Mev a noticeable discrepancy begins to appear between the measured cross sections and the resonance curve, this being explained[13] by the increasing role of non-resonant Ss transition, which is substantial near the reaction threshold. The contribution to the total cross section corresponding to this transition was found by us by comparing the values of the measured cross sections with the resonance curve, and was found to be

$$\sigma_{Ss} = (0.032 \pm 0.007)\,\eta_m^2 \cdot 10^{-27}\ cm^2.$$

Taking into account also the contribution of resonant transitions,[13] the cross section of reaction (1) near the threshold at energies less than 400 Mev can be represented in the form

$$\sigma^{\pi^0}_{pp} = (0.032\eta_m^2 + 0.040\ \eta_m^6 + 0.047\ \eta_m^8)\cdot 10^{-27}\ cm^2.$$

Here the first term is due to nonresonant Ss transition, the second to "shifted" Ss and Sd transitions, and the last one to Pp transitions. The Ps transition, which is also characterized by proportionality to η_m^6, is assumed to be insignificant in Mandel'shtam's theory. In the energy region from 450 to 600 Mev, the cross section of the investigated reaction increases at a constant rate, and varies as $\eta_m^{5.7}$. At still greater energies the increase in the cross sections slows down, in accordance with the Mandel'shtam theory (see Fig. 12).

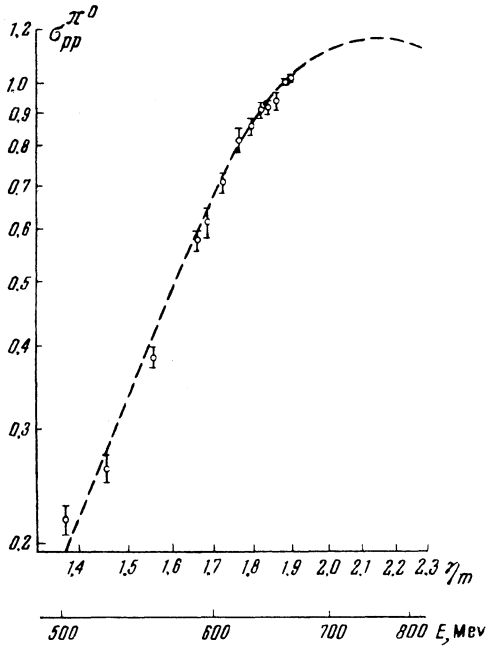

FIG. 12. Dependence of the cross section (in relative units) of reaction (1) on the momentum η_m in the region of the maximum. The experimental data and the theoretical curve, taken from reference 13, are normalized to E = 660 Mev. The errors indicated are those in the relative measurements of the energy dependence of the cross section, and are therefore less than the errors of the absolute measurements of the cross sections, given in Fig. 11.

Comparison of the cross sections for production of neutral and charged pions in proton collisions. The results of the present work and of many other investigations[25] yield information on the ratio $\pi^0/\pi^+ = \sigma^{\pi^0}_{pp}/\sigma^{\pi^+}_{pp,pn}$, where $\sigma^{\pi^+}_{pp,pn}$ is the cross section of the reaction $p + p \rightarrow p + n + \pi^+$, in the final state of which the nucleons are

not bound. At 660 Mev this ratio is

$$\pi^0/\pi^+ = 0.294 \pm 0.015.$$

The ratio π^0/π^+ was calculated by Peaslee[26] for the case when all the transitions are realized through the resonant state ($T = 3/2$, $J = 3/2$), and was found to equal $1/5$. Allowance for the interference of the nucleon states and the differences in the π-meson masses[13] modifies this quantity considerably and brings it closer to the experimental

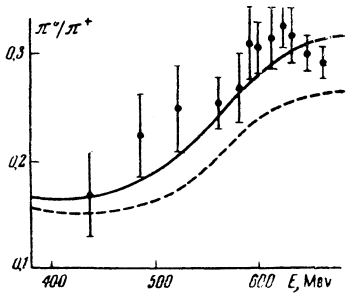

FIG. 13. Ratio of the cross sections of production of π^0 and π^+ mesons by protons at different energies. The solid curve is calculated assuming Eq. (11), while the dotted one corresponds to Eq. (10).

data. The curves shown in Fig. 13 were calculated by Mandel'shtam (private communication) with allowance for the nonresonant Ss transition. The lower curve was calculated under the assumption[13] that the three parameters, which describe P scattering in states with values of total angular momentum J = 2, 1, and 0, are equal to each other:

$$|b_{2a}| = |b_{1a}| = |b_{01}| = b_a, \qquad (10)$$

where b_a is one of the two free parameters of the P scattering in the resonance theory. This assumption was introduced in the theory in a somewhat arbitrary manner. As indicated in Mandel'shtam's private communication, a more correct assumption is

$$|b_{2a}|^2 = 2|b_{1a}|^2 = 2|b_{01}|^2, \qquad (11)$$

i.e., the production of π^0 mesons is more probable in the state with J = 2 than in the states with J = 1 and J = 0. In the latter case one observes a better agreement between the calculated ratio π^0/π^+ and the experimental data (see Fig. 13). Another circumstance in favor of relation (11) is, as indicated in a private communication by G. Braun, the small magnitude of the radius of the repelling core for the state $^3P_2$, compared with $^3P_1$ and $^3P_0$, thanks to which the production of mesons is less supressed than in the state with J = 2 in that with J = 1 and J = 0.

The quantity π^0/π^+ is thus sufficiently sensitive to the relations between various P-scattering parameters. Other characteristics of reaction (1) are less sensitive to changes in the parameter relations. Thus, the π^0-meson angular distributions calculated for the cases (10) and (11) hardly differ from each other, as can be seen from Fig. 10.

5. CONCLUSIONS

The comparison made in this paper of the experimental data with the Mandel'shtam theory shows that the accuracy with which this theory describes the main properties of the process of π^0-meson production by protons at energies E < 700 Mev is quite high. In connection with this, it is of great interest to continue further systematic investigations of this reaction at higher energies, 700 — 1000 Mev, where its cross section, according to theory, passes through a maximum. The data obtained thus far in this energy region[27] are contradictory and cannot therefore be used for comparison with the theory.

In conclusion, we take this opportunity to thank L. I. Lapidus, S. L. Mandel'shtam, L. M. Soroko, and A. A. Tyapkin for discussion of the results of the present work. We are grateful to B. M. Antonov, E. L. Grigor'ev, G. P. Zorin, M. M. Kulyukin, N. A. Mitin, O. V. Savchenko, and I. V. Tsymbulov for help in performing the measurements.

[1] A. Rosenfeld, Phys. Rev. **96**, 139 (1954).

[2] Hales, Hildebrand, Knable, and Moyer, Phys. Rev. **85**, 37 (1952).

[3] Marshall, Marshall, Nedzel, and Warshaw, Phys. Rev. **88**, 632 (1952).

[4] Pontecorvo, Selivanov, and Zhukov, Отчет ОИЯИ. (Report, Joint. Inst. for Nuclear Research, Acad. Sci. U.S.S.R.), 1952, p. 81.

[5] Kozodaev, Tyapkin, Bayukov, Markov, Prokoshkin, Izv. Akad. Nauk SSSR, Ser. Fiz. **19**, 589 (1955), Columbia Tech. Transl. p. 529.

[6] L. M. Soroko, J. Exptl. Theoret. Phys. (U.S.S.R.) **30**, 296 (1956), Soviet Phys. JETP **3**, 184 (1956).

[7] J. Mather and E. Martinelli, Phys. Rev. **92**, 749 (1953).

[8] W. Crandall, B. Moyer, Phys. Rev. **92**, 749 (1953).

[9] M. Gell-Mann and K. Watson, Ann. Rev. Nucl. Sci. **4**, 219 (1954).

[10] Tyapkin, Kozodaev, and Prokoshkin, Dokl. Akad. Nauk SSSR **100**, 689 (1955).

[11] Yu. D. Prokoshkin and A. A. Tyapkin, J. Exptl. Theoret. Phys. (U.S.S.R.) **32**, 750 (1957), Soviet Phys. JETP **5**, 618 (1957).

[12] Stallwood, Sutton, Fields, Fox, and Kane, Phys. Rev. **101**, 1716 (1958).

[13] S. Mandelstam, Proc. Roy. Soc. **A244**, 491 (1958).

[14] Yu. Prokoshkin, Proc. CERN Symposium **2**, 385 (1956); cf. data of B. D. Balashov, V. A. Zhukov, B. Pontecorvo, and G. I. Selivanov (p. 393).

[15] Yu. D. Bayukov and A. A. Tyapkin, J. Exptl. Theoret. Phys. (U.S.S.R.) **32**, 953 (1957), Soviet Phys. JETP **5**, 779 (1957).

[16] B. Moyer and R. Squire, Phys. Rev. **107**, 283 (1957).

[17] Yu. D. Prokoshkin, J. Exptl. Theoret. Phys. (U.S.S.R.) **31**, 732 (1956), Soviet Phys. JETP **4**, 618 (1957).

[18] I. M. Vasilevskiĭ and Yu. D. Prokoshkin, Атомная энергия (Atomic Energy), in press.

[19] Bayukov, Kozodaev, and Tyapkin, J. Exptl. Theoret. Phys. (U.S.S.R.) **32**, 667 (1957), Soviet Phys. JETP **5**, 552 (1957).

[20] A. A. Tyapkin, J. Exptl. Theoret. Phys. (U.S.S.R.) **30**, 1150 (1956), Soviet Phys. JETP **3**, 979 (1956).

[21] V. P. Dzhelepov and B. M. Pontecorvo, Атомная энергия (Atomic Energy) **3**, 413 (1957).

[22] A. Ashkin and R. Marshak, Phys. Rev. **76**, 58 (1949). Bjorklund, Crandall, Moyer, and York, Phys. Rev. **77**, 213 (1950).

[23] Richman, Weissbluth, and Wilcox, Phys. Rev. **85**, 161 (1952); Passman, Block, and Havens, Phys. Rev. **88**, 1247 (1952); S. Leonard, Phys. Rev. **93**, 1380 (1954); W. Dudziak, Phys. Rev. **95**, 866 (1954).

[24] Meshkovskiĭ, Pligin, Shalamov, and Shebanov, J. Exptl. Theoret. Phys. (U.S.S.R.) **32**, 1328 (1957), Soviet Phys. JETP **5**, 1085 (1957).

[25] V. S. Neganov and O. V. Savchenko, J. Exptl. Theoret. Phys. (U.S.S.R.) **32**, 1265 (1957), Soviet Phys. JETP **5**, 1033 (1957); Dzhelepov, Moskalev, and Medved', Dokl. Akad. Nauk SSSR **104**, 380 (1955); Paper delivered at Conference on High-Energy Particle Physics, Moscow, 1956. G. M. Meshcheryakov and B. S. Neganov, Dokl. Akad. Nauk SSSR **100**, 677 (1955). Fields, Fox, Kane, Stallwood, and Sutton, Phys. Rev. **109**, 1713 (1958).

[26] D. Peaslee, Phys. Rev. **95**, 1580 (1954).

[27] Hughes, March, Mirhead, and Lock, Proc. CERN Symposium **2**, 344 (1956). Morrison, Fowler, and Garrison, Phys. Rev. **103**, 1472 (1956).

Translated by J. G. Adashko
345